Numer. Math. Theor. Meth. Appl.
doi: 10.4208/nmtma.2012.m1045

Vol. **5**, No. 2, pp. 278-296
May 2012

Asymptotic Preserving Schemes for Semiconductor Boltzmann Equation in the Diffusive Regime

Jia Deng*

Department of Mathematical Sciences, Tsinghua University, Beijing 100084, P.R. China.

Received 12 December 2010; Accepted (in revised version) 1 July 2011

Available online 27 March 2012

Abstract. As is known, the numerical stiffness arising from the small mean free path is one of the main difficulties in the kinetic equations. In this paper, we derive both the split and the unsplit schemes for the linear semiconductor Boltzmann equation with a diffusive scaling. In the two schemes, the anisotropic collision operator is realized by the "BGK"-penalty method, which is proposed by Filbet and Jin [F. Filbet and S. Jin, J. Comp. Phys. 229(20), 7625-7648, 2010] for the kinetic equations and the related problems having stiff sources. According to the numerical results, both of the schemes are shown to be uniformly convergent and asymptotic-preserving. Besides, numerical evidences suggest that the unsplit scheme has a better numerical stability than the split scheme.

AMS subject classifications: 35Q20, 65M12

Key words: linear semiconductor Boltzmann equation, drift-diffusion limit, diffusive relaxation system, "BGK"-penalty method.

1. Introduction

The semiconductor Boltzmann equation, serving as the mathematical model for the highly integrated semiconductor devices, has a diffusive scaling measured by the dimensionless parameter ϵ, i.e., the ratio of the mean free path of the particle with the typical length. When ϵ goes to zero, i.e, $\epsilon \to 0^+$, the kinetic equations lead asymptotically to the drift-diffusion equations.

In practical applications, it is often found that ϵ locates in the very different scale within one problem, which causes the difficulty of transition regime, i.e, a regime with ϵ too small for the kinetic equations to avoid numerical stiffness, and meanwhile, too large for the drift-diffusion equations to be accurate [15]. In this situation, one has to resolve the kinetic scaling and applies very fine grids to the kinetic equations when using the standard numerical methods. Clearly, the cost will be expensive. On the other hand, what we are concerned is actually the macroscopic observables of the system, such as the

*Corresponding author. *Email address:* dengj04@gmail.com (Jia Deng)

mass density and the bulk momentum, but not the phase distribution [4]. Hence, it is worthless to compute the kinetic models wherever and whenever the drift-diffusion limits are valid. To tackle this problem, one can apply such a class of multiscale, multi-physics type domain decomposition methods (see, e.g., [3, 5, 7, 20]). All of them have the same idea of solving the drift-diffusion equations in the diffusive regimes (where ϵ is small), and the kinetic equations in the rarefied regimes (where ϵ is big). However, these methods have the difficulties of determining the interface, including the location and the coupling condition. In the recent years, the domain decomposition methods are gradually replaced by the so-called asymptotic-preserving (AP) schemes in many areas.

The concept of AP was firstly summarized by Jin as follows. An AP scheme should possess the discrete analogy of the continuous asymptotic limit when $\epsilon \to 0^+$ (see, e.g., [9]). To derive a class of AP schemes for the kinetic equations having the drift-diffusion limits, Jin, Pareschi and Toscani proposed the diffusive relaxation system (DRS) and described the features of the diffusive relaxation schemes as follows (see, e.g., [9–12]):

- The numerical stability is independent of ϵ. Even in the worst case, it is merely restricted by the parabolic condition $\Delta t \sim O(\Delta x^2)$.
- For the fixed step sizes Δt and Δx, when $\epsilon \to 0^+$, the scheme becomes a good solver for the limiting drift-diffusion equation.
- The collision term, though applied with the implicit scheme, can be implemented explicitly.

Here, we employ the idea of DRS and derive two diffusive relaxation schemes in three steps. Firstly, we reformulate the kinetic equation into the DRS using the even- and odd- parities (see, e.g., [10–12]). Next, we apply the upwind scheme associated with the high-resolution method to the left hand side (LHS) of DRS, which corresponds to a standard nonstiff hyperbolic system. Finally, we perform the time discretization with the split and the unsplit techniques, respectively. In both the split and the unsplit schemes, the anisotropic collision term is dealt with the "BGK"-penalty method proposed by Filbet and Jin in [6], the velocity discretization is done with a quadrature method based on the Hermite polynomials and being essentially the moment method (see, e.g., [10, 14]).

In this paper, it is the first time for the "BGK"-penalty method applied to the Boltzmann equation with a diffusive scaling. Some other related works can be found in [8, 13], where the authors have verified the efficiency of the method for the Fokker-Planck-Landau and Quantum Boltzmann equations with the Euler limit. The outline of this paper is as follows. In Section 2, we give a brief introduction for the linear semiconductor Boltzmann equation, including the associated diffusive scaling and the reformulation of the DRS. In Section 3, we arrange three parts for the numerical schemes. Part 1 gives the quadrature method for the velocity discretization. Part 2 introduces the high-resolution method for the LHS of the DRS. Part 3 presents the split and the unsplit techniques for the time discretization, including the "BGK"-penalty method for the collision term. In Section 4, we apply both the split and the unsplit schemes to two transport problems in the slab geometry. According

to the numerical results, the two schemes are shown with the AP property, and the unsplit scheme has a better numerical stability than the split scheme.

2. Linear Semiconduction Boltzmann Equation and Drift-Diffusion Limit

In this section, we arrange two parts. In part 1, we introduce the linear semiconductor Boltzmann equation and its diffusive scaling [2]. In Part 2, we perform a brief asymptotic analysis for the kinetic equation, and then reformulate it into the DRS.

2.1. The Linear Semiconduction Boltzmann Equation

Electron transport in semiconductors is usually modeled (See [1,2]) by the linear semiconductor Boltzmann equation, which has the form of

$$\partial_t f + \frac{1}{\hbar}\nabla_{\vec{k}}\mathscr{E}(\vec{k})\cdot\nabla_{\vec{x}} f + \frac{q}{\hbar}\nabla_{\vec{x}} V(\vec{x},t)\cdot\nabla_{\vec{k}} f = \mathscr{Q}(f). \tag{2.1}$$

Here $\vec{k}\in\mathbb{B}$ is the wave vector in the first Brillouin zone $\mathbb{B}$, which is associated with the lattice structure, $\vec{x}\in\Omega$ is the electron position in the computational domain $\Omega\subset\mathbb{R}^3$, $t\in\mathbb{R}^+$ is the time variable, and $f=f(\vec{x},\vec{k},t)$ is the space phase density distribution. The two constants $q>0$ and $\hbar$ denote the electron charge and the reduced Plank's constant, respectively. $\mathscr{E}(\vec{k})$ stands for a given energy band diagram, and $V(\vec{x},t)$ is the external potential. In this paper, we treat $V(x,t)$ as a given function independent of t, i.e., $V(x,t)=V(x)$. The collision operator $\mathscr{Q}$ for elastic collisions is given by

$$\mathscr{Q}(f)(\vec{k}) = \int_{\mathbb{B}} \sigma(\vec{k},\vec{k}')f(\vec{k}')\mathrm{d}\vec{k}'\mathscr{M}(\vec{k})\mathscr{M}(\vec{k}) - \lambda(\vec{k})f(\vec{k}),$$
$$\mathscr{M}(\vec{k}) = \exp(-\frac{\mathscr{E}(\vec{k})}{K_B T_0}), \quad \lambda(\vec{k}) = \int_{\mathbb{R}^3}\sigma(\vec{k},\vec{k}')\mathscr{M}(\vec{k}')\mathrm{d}\vec{k}',$$

where $\mathscr{M}(\vec{k})$ is the Maxwellian depending on the Boltzmann constant K_B and the thermal temperature T_0, $\lambda(\vec{k})$ denotes the collision frequency, and $\sigma(\vec{k},\vec{k}')$ is the cross section being assumed with the properties as

- Rotation invariance: $\forall\ \mathscr{R}\in\mathbb{SO}(3)$, it holds $\sigma(\mathscr{R}\vec{k},\mathscr{R}\vec{k}')=\sigma(\vec{k},\vec{k}')$;
- Symmetry: $\forall\ \vec{k},\vec{k}'\in\mathbb{B}$, it holds $\sigma(\vec{k},\vec{k}')=\sigma(\vec{k}',\vec{k})$;
- Boundedness: $\exists\ c_0,c_1>0$, such that $c_0\le\sigma(\vec{k},\vec{k}')\le c_1$.

As usual, we begin with rescaling equation (2.1) (See [2], [19]). For simplicity, we consider the local parabolic approximation, i.e., $\mathscr{E}(\vec{k})=\frac{\hbar^2}{2m}|\vec{k}|^2$, where m is the effective mass. In this case, the definition domain of $\vec{k}$ can be extended from $\mathbb{B}$ to the whole space $\mathbb{R}^3$. Let x_0 be the typical length of the system, and $\mathscr{E}_0=K_BT_0$ be the typical kinetic energy. Then the wave vector scale k_0, the time scale t_0, the potential scale V_0, the Maxwellian scale M_0,

the distribution scale f_0, the cross section scale σ_0, and the collision frequency scale λ_0 satisfy

$$k_0 = \frac{\sqrt{2m\mathscr{E}_0}}{\hbar},\ t_0 = \frac{mx_0}{\hbar k_0},\ \ V_0 = \frac{2\mathscr{E}_0}{q},$$
$$M_0 = \sqrt{\pi}^3,\ \ f_0 = \frac{1}{x_0^3 k_0^3},\ \ \lambda_0 = \sigma_0 M_0 k_0^3.$$

By introducing the dimensionless arguments

$$\vec{k}_s = \frac{\vec{k}}{k_0},\quad \vec{x}_s = \frac{\vec{x}}{x_0},\quad t_s = \frac{t}{t_0},$$

and the Knudsen number $\epsilon = \frac{1}{\lambda_0 t_0}$, the dimensionless form of equation (2.1) is give as

$$\partial_{t_s} f_s + \vec{k}_s \cdot \nabla_{\vec{x}_s} f_s + \nabla_{\vec{x}_s} V_s \cdot \nabla_{\vec{k}_s} f_s = \frac{1}{\epsilon} \mathscr{Q}_s(f_s), \tag{2.2}$$

where

$$V_s(\vec{x}_s) = \frac{V(x_0\vec{x}_s)}{V_0},\ \ \mathscr{M}_s(\vec{k}_s) = \frac{\mathscr{M}(k_0\vec{k}_s)}{M_0},\ \ f_s(\vec{x}_s, \vec{k}_s, t_s) = \frac{f(x_0\vec{x}_s,\, k_0\vec{k}_s,\, t_0 t_s)}{f_0},$$
$$\sigma_s(\vec{k}_s, \vec{k}_s') = \frac{\sigma(k_0\vec{k}_s,\, k_0\vec{k}_s')}{\sigma_0},\ \ \lambda_s(\vec{k}_s) = \frac{\lambda(k_0\vec{k}_s)}{\lambda_0},\ \ \mathscr{Q}_s(\cdot)(\vec{k}_s) = \frac{\mathscr{Q}(\cdot)(k_0\vec{k}_s)}{\lambda_0}.$$

For the more general case, we assume the Knudsen number depending on the position variable, i,e., $\epsilon = \epsilon(\vec{x}_s)$, and define the constant $\delta = \max_{\vec{x}_s \in \Omega} \epsilon(\vec{x}_s)$. When $\delta \ll 1$, the equation (2.2) leads a diffusive scaling with

$$t' = \delta t_s,\ \ \vec{v}' = \vec{k}_s,\ \ \vec{x}' = \vec{x}_s,$$

and thus

$$\partial_t f + \frac{1}{\delta}\left(\vec{v} \cdot \nabla_{\vec{x}} f - \vec{E} \cdot \nabla_{\vec{v}} f\right) = \frac{\mathscr{Q}(f)}{\epsilon\delta}. \tag{2.3}$$

Here all the primes have been omitted, $\vec{v}$ denotes the velocity of the electron, $\vec{E}(\vec{x}) = -\nabla_{\vec{x}} V(\vec{x})$ is the external field with $\|\vec{E}(\vec{x})\|_{L^\infty(\Omega)}$ bounded, and the rescaled collision operator $\mathscr{Q}$ is connected with velocity $\vec{v}$ through

$$\mathscr{Q}(f)(\vec{v}) = \int_{\mathbb{R}^3} \sigma(\vec{v}, \vec{v}') f(\vec{v}') \mathrm{d}\vec{v}' \mathscr{M}(\vec{v}) - \lambda(\vec{v}) f(\vec{v}),,$$
$$\mathscr{M}(\vec{v}) = \frac{1}{\sqrt{\pi}^3} \exp(-|\vec{v}|^2), \quad \lambda(\vec{v}) = \int_{\mathbb{R}^3} \sigma(\vec{v}, \vec{v}') \mathscr{M}(\vec{v}') \mathrm{d}\vec{v}'.$$

2.2. The Drift-Diffusion Limit

It is well-known that the phase distribution f contains all the information about the macroscopic observables, such as the mass density ρ and the bulk momentum $\vec{u}$ through the relations

$$\rho(\vec{x},t)=\int_{\mathbb{R}^3} f(\vec{x},\vec{v},t)\mathrm{d}\vec{v}\,,\quad \vec{u}(\vec{x},t)=\int_{\mathbb{R}^3}\vec{v}f(\vec{x},\vec{v},t)\mathrm{d}\vec{v}\,. \tag{2.4}$$

However, since f depends on seven variables, thus it is challenging for the storage device. One preferred approach is deducing some approximate macroscopic model through asymptotic analysis [4]. In this subsection, a brief asymptotic analysis is given for the equation (2.3), which suggests the kinetic model having the drift-diffusion limit in the sense of $\delta\to 0^+$. As a preliminary, we present several standard theoretical results (See [2, 17–19]) for the collision operator $\mathscr{Q}$.

Theorem 2.1. *Denote the Hilbert space $\mathscr{H}=\mathscr{L}^2\big(\mathbb{R}^3;\mathrm{d}\vec{v}/\mathscr{M}(\vec{v})\big)$. Then it holds that*

1. *$-\mathscr{Q}$ is bounded and self-adjoint.*
2. *$Ker\mathscr{Q}$=$Span\{\mathscr{M}(\vec{v})\}\subset\mathscr{H}$, $Ran\mathscr{Q}$=$Ker\mathscr{Q}^{\perp}$.*
3. *There exists a constant $\tilde{c}_0>0$ such that*

$$-\big\langle\mathscr{Q}(f),f\big\rangle_{\mathscr{H}}\geq\tilde{c}_0\|f-\mathscr{P}(f)\|^2_{\mathscr{H}},\quad\forall f\in\mathscr{H},$$

where

$$\big\langle\mathscr{Q}(f),f\big\rangle_{\mathscr{H}}=\int_{\mathbb{R}^3}\frac{\mathscr{Q}(f)(\vec{v})f(\vec{v})}{\mathscr{M}(\vec{v})}\mathrm{d}\vec{v},\quad\mathscr{P}(f)=\int_{\mathbb{R}^3}f\,\mathrm{d}\vec{v}\mathscr{M}(\vec{v})\,.$$

4. *Let $\vec{h}=\vec{h}(\vec{v})\in\mathbb{R}^3$ be the unique solution to $\mathscr{Q}(\vec{h})=\mathscr{M}(\vec{v})\vec{v}$ in* Ran$\mathscr{Q}$. *Then $\vec{h}$ is an odd function of $\vec{v}$ and there exists a positive number μ such that $\int_{\mathbb{R}^3}\vec{v}\otimes\vec{h}\mathrm{d}\vec{v}=-\mu\mathbf{I}_{3\times3}$. μ is called the mobility.*

Given the even and odd parities

$$r(\vec{x},\vec{v},t)=\frac{1}{2}[f(\vec{x},\vec{v},t)+f(\vec{x},-\vec{v},t)], \tag{2.5a}$$

$$j(\vec{x},\vec{v},t)=\frac{1}{2\delta}[f(\vec{x},\vec{v},t)-f(\vec{x},-\vec{v},t)], \tag{2.5b}$$

it is straightforward that

$$r(\vec{v})=r(-\vec{v}),\quad j(\vec{v})=-j(-\vec{v}),\quad\mathscr{Q}(j)=-\lambda j\,, \tag{2.6a}$$

$$\rho(\vec{x},t)=\int_{\mathbb{R}^3}r(\vec{x},\vec{v},t)\mathrm{d}\vec{v},\quad\vec{u}(\vec{x},t)=\delta\int_{\mathbb{R}^3}\vec{v}j(\vec{x},\vec{v},t)\mathrm{d}\vec{v}\,. \tag{2.6b}$$

For simplicity, we consider the uniform regime in Ω. When $\delta \ll 1$, suppose f has the following Hilbert expansion form

$$f = f_0 + \delta f_1 + \delta^2 f_2 + \cdots . \tag{2.7}$$

Inserting (2.7) into (2.3) and equating the different powers of δ, one gets

$$O(\delta^{-1}): \quad \mathcal{Q}(f_0) = 0 , \tag{2.8a}$$
$$O(\delta^{0}): \quad \mathcal{Q}(f_1) = \vec{v}\cdot\nabla_{\vec{x}} f_0 - \vec{E}\cdot\nabla_{\vec{v}} f_0 , \tag{2.8b}$$
$$O(\delta^{1}): \quad \mathcal{Q}(f_2) = \partial_t f_0 + \vec{v}\cdot\nabla_{\vec{x}} f_1 - \vec{E}\cdot\nabla_{\vec{v}} f_1 , \tag{2.8c}$$
$$O(\delta^{2}): \quad \mathcal{Q}(f_3) = \partial_t f_1 + \vec{v}\cdot\nabla_{\vec{x}} f_2 - \vec{E}\cdot\nabla_{\vec{v}} f_2 . \tag{2.8d}$$

Applying the Theorem 2.1-(ii) to equation (2.8a), f_0 is solved as $f_0 = \rho_0 \mathcal{M}(\vec{v})$, which implies $r_0 = \rho_0 \mathcal{M}(\vec{v})$ and $j_0 = 0$. Splitting $\vec{v}$ in (2.8b) into $\vec{v}$ and $-\vec{v}$, one gets

$$\mathcal{Q}(f_1)(\vec{v}) = \vec{v}\cdot\nabla_{\vec{x}} f_0 - \vec{E}\cdot\nabla_{\vec{v}} f_0, \quad \mathcal{Q}(f_1)(-\vec{v}) = -\vec{v}\cdot\nabla_{\vec{x}} f_0 + \vec{E}\cdot\nabla_{\vec{v}} f_0 .$$

Adding and subtracting the two equations above, r_1 and j_1 are solved as

$$r_1 = \rho_1 \mathcal{M}(\vec{v}), \quad \delta j_1 = \vec{h}(\vec{v})\cdot(\nabla_{\vec{x}}\rho_0 + 2\rho_0 \vec{E}),$$

where the property (2.6) and the Theorem 2.1-(iv) are used. The solvability of (2.8c) suggests

$$\int_{\mathbb{R}^3} (\partial_t f_0 + \vec{v}\cdot\nabla_{\vec{x}} f_1 - \vec{E}\cdot\nabla_{\vec{v}} f_1)\,\mathrm{d}\vec{v} = 0 .$$

Since

$$\begin{aligned}
&\int_{\mathbb{R}^3} (\vec{v}\cdot\nabla_{\vec{x}} f_1 - \vec{E}\cdot\nabla_{\vec{v}} f_1)\mathrm{d}\vec{v} \\
=&\nabla_{\vec{x}}\cdot\left(\int_{\mathbb{R}^3} \delta\vec{v} j_1 \mathrm{d}\vec{v}\right) = \nabla_{\vec{x}}\cdot\left(\int_{\mathbb{R}^3} \vec{v}\otimes\vec{h}(\vec{v})\mathrm{d}\vec{v}\cdot(\nabla_{\vec{x}}\rho_0 + 2\rho_0\vec{E})\right) \\
=&-\nabla_{\vec{x}}\cdot\mu(\nabla_{\vec{x}}\rho_0 + 2\rho_0\vec{E}),
\end{aligned}$$

thus ρ_0 satisfies the following drift-diffusion equation

$$\partial_t\rho_0 - \nabla_{\vec{x}}\cdot\mu(\nabla_{\vec{x}}\rho_0 + 2\rho_0\vec{E}) = 0 ,$$

with the mobility μ. Analogously, one can derive ρ_1 fulfilling the same drift-diffusion equation as ρ_0. Hence, it establishes

$$\partial_t\rho - \nabla_{\vec{x}}\cdot\mu(\nabla_{\vec{x}}\rho + 2\rho\vec{E}) = O(\delta^2). \tag{2.9}$$

In this paper, we assume $\delta \le 1$.

3. Numerical Scheme

We simply consider one-dimensional schemes in this section. According to [11, 12], even when the anisotropic collision term is treated efficiently, solving (2.3) directly is still restricted to the best Courant-Friedrichs-Levy (CFL) condition, i.e.,$\Delta t \sim O(\delta \Delta x)$. Consequently, the cost is still expensive when $\delta \ll 1$. To tackle this problem, we follow the idea in [10–12], and reformulate (2.3) into the system with respect to the parities (2.5), i.e.,

$$\partial_t r + v_1 \partial_x j - E \partial_{v_1} j = \frac{\mathcal{Q}(r)}{\epsilon \delta}, \tag{3.1a}$$

$$\partial_t j + \frac{v_1 \partial_x r - E \partial_x r}{\delta^2} = -\frac{\lambda j}{\epsilon \delta}. \tag{3.1b}$$

Here v_1 denotes the first component of velocity $\vec{v} = (v_1, v_2, v_3)$. Next, we rewrite (3.1a)-(3.1b) into the DRS, i.e.,

$$\partial_t r + v_1 \partial_x j - E \partial_{v_1} j = \frac{\mathcal{Q}(r)}{\epsilon \delta}, \tag{3.2a}$$

$$\partial_t j + \phi(v_1 \partial_x r - E \partial_{v_1} r) = -\frac{1}{\epsilon \delta}[\lambda j + \frac{\epsilon(1-\delta^2)}{\delta}(v_1 \partial_x r - E \partial_{v_1} r)], \tag{3.2b}$$

where the artificial parameter ϕ is restricted by the relation $0 \le \phi \le \frac{1}{\delta^2}$ to ensure the problem being well-posed uniformly with δ. Since we have assumed $\delta \le 1$, thus we simply set $\phi = 1$. The following split and the unsplit schemes are all based on the DRS (3.2a)-(3.2b), moreover, except the time discretization they have the velocity discretization, the LHS of the DRS and the anisotropic collision term discretized in the same manners.

3.1. Velocity Discretization

The quadrature method utilizes the Hermite polynomial and be essentially the moment method. According to [18, 19], the method is stable and has the spectral accuracy. As a preliminary, we introduce some notations. Given the triple indexes (See [14, 18, 19]) $\mathbf{l} = (l_1, l_2, l_3)$, $l_1, l_2, l_3 \in \mathbb{Z}_0^+$, and $\mathbf{m} = (m_1, m_2, m_3)$, $m_1, m_2, m_3 \in \mathbb{Z}_0^+$, the velocity node is written as $\vec{v}^{\mathbf{l}} = (v_1^{l_1}, v_2^{l_2}, v_3^{l_3})$, and the function $h_{\mathbf{m}}(\vec{v})$ denotes

$$h_{\mathbf{m}}(\vec{v}) = h_{m_1}(v_1) h_{m_2}(v_2) h_{m_3}(v_3),$$

where the one dimensional Hermite polynomial $h_{m_i}(v_i)$, $v_i \in \mathbb{R}$, $i = 1, 2, 3$, satisfies

$$h_{-1}(v_i) = 0, \quad h_0(v_i) = \pi^{-1/4}, \tag{3.3a}$$

$$h_{m_i+1}(v_i) = v_i \sqrt{\frac{2}{m_i+1}} h_{m_i}(v_i) - \sqrt{\frac{m_i}{m_i+1}} h_{m_i-1}(v_i), \ \ m_i \ge 0, \tag{3.3b}$$

$$h'_{m_i}(v_i) = \sqrt{2 m_i}\, h_{m_i-1}(v_i). \tag{3.3c}$$

Clearly, the series $\{h_{\mathbf{m}}(\vec{v})\mathscr{M}(\vec{v})\}_{\mathbf{m}}$ consists of an orthonormal basis of the Hilbert space $\mathscr{H}$. From the aspect of numerical implementations, it generally truncates the orthonormal basis for a specified triple index $\mathbf{M}=(M_1,M_2,M_3)$, $M_1,M_2,M_3\in\mathbb{Z}^+$. Next, as was done in [10,14], we factor the Maxwellian from the parities and rewrite them into the forms of

$$r=\varphi(\vec{x},\vec{v},t)\mathscr{M}(\vec{v}),\quad j=\psi(\vec{x},\vec{v},t)\mathscr{M}(\vec{v}), \tag{3.4}$$

where

$$\varphi=\sum_{0\le\mathbf{m}\le\mathbf{M}}\varphi_{\mathbf{m}}(\vec{x},t)h_{\mathbf{m}}(\vec{v}),\quad \psi=\sum_{0\le\mathbf{m}\le\mathbf{M}}\psi_{\mathbf{m}}(\vec{x},t)h_{\mathbf{m}}(\vec{v}).$$

It is straightforward that

$$\partial_{v_1}r=\mathscr{M}\partial_{v_1}\varphi-2v_1\varphi\mathscr{M},\quad \partial_{v_1}j=\mathscr{M}\partial_{v_1}\psi-2v_1\psi\mathscr{M}.$$

Since the term $\partial_{v_1}j$ is discretized in the same manner as $\partial_{v_1}r$, thus we consider $\partial_{v_1}r$ only. Using the property (3.3c), one gets

$$\partial_{v_1}\varphi=\sum_{0\le\mathbf{m}\le\mathbf{M}-\mathbf{e}_1}\sqrt{2(m_1+1)}\varphi_{\mathbf{m}+\mathbf{e}_1}h_{\mathbf{m}}(\vec{v}), \tag{3.5}$$

with $\mathbf{e}_1=(1,0,0)$. On the other hand, owing to the relation

$$\varphi_{\mathbf{m}}=\int_{\mathbb{R}^3}\varphi(\vec{v}')h_{\mathbf{m}}(\vec{v}')e^{-|\vec{v}'|^2}\mathrm{d}\vec{v}'=\sum_{0\le\mathbf{l}\le\mathbf{M}}\varphi(\vec{v}^{\mathbf{l}})h_{\mathbf{m}}(\vec{v}^{\mathbf{l}})\omega^{\mathbf{l}},$$

one can reduce (3.5) to be as

$$\partial_{v_1}\varphi(\vec{v})=\sum_{0\le\mathbf{m}\le\mathbf{M}-\mathbf{e}_1}\sqrt{2(m_1+1)}h_{\mathbf{m}}(\vec{v})h_{\mathbf{m}+\mathbf{e}_1}(\vec{v}^{\mathbf{l}})\omega^{\mathbf{l}}_{\mathbf{m}+\mathbf{e}_1}\varphi(\vec{v}^{\mathbf{l}}),$$

where $v_1^{l_1},v_2^{l_2},v_3^{l_3}$, $l_1,l_2,l_3\in\mathbb{Z}_0^+$, are the roots of Hermite polynomials $h_{M_1+1}(v)$, $h_{M_2+1}(v)$, $h_{M_3+1}(v)$, respectively, and $\omega^{\mathbf{l}}$ is the associated weight given by

$$\omega^{\mathbf{l}}=\prod_{i=1}^{3}\frac{1}{(M_i+1)h^2_{M_i}(v_i^{l_i})}. \tag{3.6}$$

Finally, the collision term is realized as

$$\begin{aligned}\mathscr{Q}(r)(\vec{v}) &= \mathscr{M}(\vec{v})\int_{\mathbb{R}^3}\sigma(\vec{v},\vec{v}')\varphi(\vec{v}')\mathscr{M}(\vec{v}')\mathrm{d}\vec{v}'-\lambda(\vec{v})r(\vec{v})\\ &= \pi^{-3/2}\mathscr{M}(\vec{v})\sum_{0\le\mathbf{l}\le\mathbf{M}}\sigma(\vec{v},\vec{v}^{\mathbf{l}})\varphi(\vec{v}^{\mathbf{l}})\omega^{\mathbf{l}}-\lambda(\vec{v})r(\vec{v}),\end{aligned}$$

with

$$\lambda(\vec{v})=\int_{\mathbb{R}^3}\sigma(\vec{v},\vec{v}')\mathscr{M}(\vec{v}')\mathrm{d}\vec{v}'=\pi^{-3/2}\sum_{0\le\mathbf{l}\le\mathbf{M}}\sigma(\vec{v},\vec{v}^{\mathbf{l}})\omega^{\mathbf{l}}.$$

3.2. Space Discretization

In this section, we introduce the high-resolution method for the space discretization of the LHS of (3.2a)-(3.2b). Setting $u = r + j$ and $w = r - j$, one gets

$$\partial_t u + v_1 \partial_x u = 0, \quad \partial_t w - v_1 \partial_x w = 0\,. \tag{3.7}$$

Without the loss of generality, we let $\Omega = [0,1]$, and simply employ a uniform mesh with grid points $x_i = i\Delta x$, $\Delta x = 1/N$, $i = 1,2,\cdots,N$, $N \in \mathbb{Z}^+$. Then the grid functions are defined by

$$r_i^n = \frac{1}{\Delta x}\int_{x_{i-\frac{1}{2}}}^{x_{i+\frac{1}{2}}} r(x,\vec{v},t^n)\mathrm{d}x, \quad j_i^n = \frac{1}{\Delta x}\int_{x_{i-\frac{1}{2}}}^{x_{i+\frac{1}{2}}} j(x,\vec{v},t^n)\mathrm{d}x\,.$$

An explicit discretization for (3.7) is given as

$$\frac{u_i^{n+1}-u_i^n}{\Delta t} + v_1\Delta_x^u u_i^n = 0, \quad \frac{w_i^{n+1}-w_i^n}{\Delta t} - v_1\Delta_x^u w_i^n = 0\,,$$

where the upwind operator Δ_x^u has the form of

$$\Delta_x^u u_i = \frac{u_{i+\frac{1}{2}} - u_{i-\frac{1}{2}}}{\Delta x}\,. \tag{3.8}$$

By a direct calculation, one has

$$r_i^{n+1} = r_i^n - \frac{v_1\Delta t\Delta_x^u j_i^n}{2}, \quad j_i^{n+1} = j_i^n - \frac{v_1\Delta t\Delta_x^u r_i^n}{2}\,. \tag{3.9}$$

Owing to the symmetry (2.6) of the parities, we consider the situation of $v_1 > 0$ only. The first order upwind scheme for (3.9) is given as

$$r_{i+\frac{1}{2}} = \frac{1}{2}(u_i + w_{i+1}), \quad j_{i+\frac{1}{2}} = \frac{1}{2}(u_i - w_{i+1}).$$

To improve the accuracy up to $O(\Delta t + \Delta x^2)$, the second order total variation diminishing (TVD) method [16] is applied as

$$r_{i+\frac{1}{2}} = \frac{1}{2}(u_i + w_{i+1}) + \frac{1}{4}(\Delta x + v_1\Delta t)[\Phi(u^+_{i+\frac{1}{2}}) - \Phi(w^-_{i+\frac{1}{2}})], \tag{3.10a}$$

$$j_{i+\frac{1}{2}} = \frac{1}{2}(u_i - w_{i+1}) + \frac{1}{4}(\Delta x + v_1\Delta t)[\Phi(u^+_{i+\frac{1}{2}}) - \Phi(w^-_{i+\frac{1}{2}})], \tag{3.10b}$$

where $\Phi(\theta)$ is the van Leer limiter given by

$$\Phi(\theta) = \frac{|\theta| + \theta}{1 + |\theta|}\,, \tag{3.11}$$

$$u^+_{i+\frac{1}{2}} = \frac{u_i - u_{i-1}}{u_{i+1} - u_i}, \quad w^-_{i+\frac{1}{2}} = \frac{w_{i+1} - w_i}{w_{i+2} - w_{i+1}}. \tag{3.12}$$

3.3. Time Discretizations

We arrange two parts for this subsection. In part 1, we introduce the split scheme. In part 2, we presents the unsplit scheme. In the two schemes, the collision terms are treated with the "BGK"-penalty method [6].

3.3.1. Time-Splitting Method

A natural way to split (3.2a)-(3.2b) is splitting it into a stiff relaxation step

$$\partial_t r = \frac{\mathcal{Q}(r)}{\epsilon\delta}, \tag{3.13a}$$

$$\partial_t j = -\frac{1}{\epsilon\delta}\left[\lambda j + \frac{\epsilon(1-\delta^2)}{\delta}(v_1\partial_x r - E\partial_{v_1} r)\right], \tag{3.13b}$$

and a nonstiff convection step

$$\partial_t r + v_1\partial_x j - E\partial_{v_1} j = 0, \tag{3.14a}$$

$$\partial_t j + v_1\partial_x r - E\partial_{v_1} r = 0. \tag{3.14b}$$

Clearly, the nonstiff convection step can be solved using the explicit high resolution method in subsection 3.2. Whereas, the stiff relaxation step should be solved by using the explicit-implicit (IMEX) scheme to ensure the δ-independent stability when $\Delta t \gg \delta$. Here the complete implicit scheme for the relaxation step will cause expensive cost due to the anisotropic collision operator [11, 12]. For example, the first order Backward Euler method applied to (3.13a)-(3.13b) gives r_i^* and j_i^* as (See [10])

$$\frac{r_i^* - r_i^n}{\Delta t} = \frac{\mathcal{Q}(r_i^*)}{\epsilon_i\delta}, \tag{3.15a}$$

$$\frac{j_i^* - j_i^n}{\Delta t} = -\frac{1}{\epsilon_i\delta}[\,\lambda j_i^* + \beta(v_1\Delta_{2x} r_i^* - E_i\partial_{v_1} r_i^*)\,], \tag{3.15b}$$

where the constant β and the central difference operator Δ_{2x}^c are defined by

$$\beta = \frac{\epsilon_i(1-\delta^2)}{\delta}, \quad \Delta_{2x}^c r_i = \frac{r_{i+1} - r_{i-1}}{2\Delta x}. \tag{3.16}$$

It is straightforward that (3.15b) can be solved explicitly with r_i^* known. However, in (3.15a), we have to invert the anisotropic $\mathcal{Q}$ and solve the algebraic system iteratively, which is costly. To ensure both the stability and the efficiency, we follow the idea of AP scheme, and utilize the "BGK"-penalty method, which is supposed by Filbet and Jin in [6] and has the ability of solving the implicit collision term explicitly. In this method, one needs to introduce an operator $\mathcal{B}$ in the "BGK" form

$$\mathcal{B}(r) = L(\rho\mathcal{M} - r), \tag{3.17}$$

where the constant L depends on the spectrum of $D\mathscr{Q}(\rho\mathscr{M})$, the Fréchet derivative of $\mathscr{Q}$. Then rewriting (3.13a) into an equivalent form as

$$\partial_t r = \frac{\mathscr{Q}(r)-\mathscr{B}(r)}{\epsilon\delta} + \frac{\mathscr{B}(r)}{\epsilon\delta}, \tag{3.18}$$

one finds that the first term on the right hand side of (3.18) has been less or even not stiff compared to the second term owing to the relation around $r \approx \rho\mathscr{M}$, i.e.,

$$\mathscr{Q}(r) \approx \mathscr{Q}(\rho\mathscr{M}) + D\mathscr{Q}(\rho\mathscr{M})(r-\rho\mathscr{M}) + \cdots.$$

Thus the first order IMEX for (3.13a) is given as

$$\frac{r_i^* - r_i^n}{\Delta t} = \frac{\mathscr{Q}(r_i^n)-\mathscr{B}(r_i^n)}{\epsilon_i\delta} + \frac{\mathscr{B}(r_i^*)}{\epsilon_i\delta}. \tag{3.19}$$

Integrating (3.19) with velocity variable over $\mathbb{R}^3$, one obtains $\rho_i^* = \rho_i^n$, which leads

$$r_i^* = r_i^n + \Delta t\tau_i\mathscr{Q}(r_i^n), \quad \tau_i = (L\Delta t + \epsilon_i\delta)^{-1}. \tag{3.20}$$

Applying (3.20) to (3.15b), j_i^* is solved as

$$j_i^* = \epsilon_i\eta_i[\delta j_i^n - \beta\nu_1\Delta t\Delta_{2x}^c r_i^* + \beta\Delta t E_i\partial_{v_1} r_i^*], \quad \eta_i = (\lambda\Delta t + \epsilon_i\delta)^{-1}. \tag{3.21}$$

The split scheme, i.e.,(3.20)-(3.21) and (3.10)-(3.12), has the accuracy of $O(\Delta t + \Delta x^2)$. In this problem, a seconder order accuracy in time is actually unnecessary owing to the parabolic CFL condition $\Delta t \sim O(\Delta x^2)$ for small δ.

3.3.2. Time-Unsplitting method

In this subsection, we perform the time discretization for (3.2a)-(3.2b) using the unsplit method. As was done in the split method, we introduce the operator $\mathscr{B}$ defined by (3.17), and rewrite (3.2a) to be as

$$\partial_t r + \nu_1\partial_x j - E\partial_{v_1} j = \frac{\mathscr{Q}(r)-\mathscr{B}(r)}{\epsilon\delta} + \frac{\mathscr{B}(r)}{\epsilon\delta}. \tag{3.22}$$

Applying the first order IMEX to (3.22) following

$$\frac{r_i^{n+1}-r_i^n}{\Delta t} + \nu_1\Delta_x^u j_i^n - E_i\partial_{v_1} j_i^n = \frac{\mathscr{Q}(r_i^n)-\mathscr{B}(r_i^n)}{\epsilon_i\delta} + \frac{\mathscr{B}(r_i^{n+1})}{\epsilon_i\delta}, \tag{3.23}$$

one gets

$$\begin{aligned} r_i^{n+1} =& r_i^n + \Delta t\tau_i\mathscr{Q}(r_i^n) + L\Delta t\tau_i(\rho_i^{n+1}-\rho_i^n)\mathscr{M} \\ & - \epsilon_i\delta\Delta t\tau_i(\nu_1\Delta_x^u j_i^n - E_i\partial_{v_1} j_i^n). \end{aligned} \tag{3.24}$$

Integrating (3.23) with velocity variable over $\mathbb{R}^3$, one obtains

$$\rho_i^{n+1} = \rho_i^n - \alpha_1 \int_{\mathbb{R}^3} v_1 \Delta_x^u j_i^n \mathrm{d}\vec{v}, \tag{3.25}$$

with which and (3.24) one can solve r_i^{n+1}. Next, we apply the first order IMEX to (3.2b) following

$$\frac{j_i^{n+1} - j_i^n}{\Delta t} + v_1 \Delta_x^u r_i^n - E_i \partial_{v_1} r_i^n = -\frac{\lambda j_i^{n+1} + \beta(v_1 \Delta_{2x}^c r_i^{n+1} - E_i \partial_{v_1} r_i^{n+1})}{\epsilon_i \delta},$$

and get

$$\begin{aligned} j_i^{n+1} =& \epsilon_i \delta \eta_i [j_i^n - \Delta t (v_1 \Delta_x^u r_i^n - E_i \partial_{v_1} r_i^n)] \\ & - \beta \Delta t \eta_i (v_1 \Delta_{2x}^c r_i^{n+1} - E_i \partial_{v_1} r_i^{n+1}). \end{aligned} \tag{3.26}$$

4. Numerical Examples

In this section, we apply both the split and the unsplit schemes to two transport problems in the slab geometry. As mentioned above, the velocity discretization is done with the quadrature method in Subsection 3.1. By numerical tests, the solution using larger M is comparable to the results using $\mathbf{M} = (16, 16, 16)$, so we only present the results using $M = 16$. The boundary conditions are assumed to be periodic. The cross section is given as either the relaxation time approximation (RTA), i.e., $\sigma(\vec{v}, \vec{w}) = 1$, or the mixture of RTA and the electron-phonon interactions (EPI) models, i.e.,

$$\sigma(\vec{v}, \vec{w}) = 1 + \mathscr{M}(\vec{v}) \tilde{\delta}(|\vec{v}|^2 - |\vec{w}|^2 + 1) + \mathscr{M}(\vec{w}) \tilde{\delta}(|\vec{v}|^2 - |\vec{w}|^2 - 1), \tag{4.1}$$

where $\tilde{\delta}(x) = \exp(-|x|^2)$ is the regularized delta function (see [11]).

In the numerical results, we use some notations as follows.

- Let $\|f\|_1$ be the discrete l^1 norm of the distribution $f = \alpha(\vec{x}, \vec{v}, t)\mathscr{M}(\vec{v}) \in \mathscr{H}$. It is calculated according to

$$\|f\|_1 = \frac{1}{N} \sum_{i=0}^{N-1} \sum_{0 \le \mathbf{l} \le \mathbf{M}} |\alpha(x_i, \vec{v}^{\mathbf{l}})| \omega^{\mathbf{l}}.$$

  where the associated weight $\omega^{\mathbf{l}}$ is given by (3.6).

- Let $\|\rho\|_{1,x}$ be the discrete l^1 norm of the function $\rho = \rho(x, t)$. It is calculated through

$$\|\rho\|_{1,x} = \frac{1}{N} \sum_{i=0}^{N-1} |\rho(x_i)|.$$

- $\{r_{ref},\ \rho_{ref}\}$ denote the reference solutions, which are obtained by using the split scheme with very fine grids. In this case, the parameter L in (3.17) is set as $L=0$, and the BGK-penalty method is not applied to the collision term. $\{r_s,\ \rho_s\}$ and $\{r_u,\ \rho_u\}$ denote the approximate solutions, which are obtained by using the split and the unsplit schemes with coarse grids, respectively. ρ_D denotes the solution to the drift-diffusion equation (2.9). The initial condition and the mobility function are given as

$$\rho_D(x,0)=\int_{\mathbb{R}^3}\varphi(x,\vec{v},0)\mathscr{M}(\vec{v})\mathrm{d}\vec{v},\quad \tilde{\mu}(x)=\frac{\epsilon(x)}{\delta}\int_{\mathbb{R}}\frac{v_1^2\mathscr{M}(\vec{v})}{\lambda(\vec{v})}\mathrm{d}\vec{v}.$$

From the numerical results, we observe the following properties of

- The unsplit method has a better numerical stability than the split method.
- Both the methods are uniformly second order, w.r.t., Δx.
- When the system has approached the global equilibrium state, the deviation $\|r_s-\rho_s\mathscr{M}\|_1$ is about first order, w.r.t., Δt, in the case of $\delta\ll 1$ and $\Delta t\gg\delta^2$, however, the deviation $\|r_u-\rho_u\mathscr{M}\|_1$ is nearly independent of Δt and about second order, w.r.t., δ.

As a conclusion, the two schemes are AP.

Example 1. In this example, we consider the uniform regime, i.e.,$\epsilon(x)=\delta$, in the computational domain $x\in[0,1]$. The electric field is given by

$$E(x,t)=\sin(2\pi x). \tag{4.2}$$

According to the numerical results in Table. 1 and Fig. 1- 5, we observe the features (i)-(iii).

In Table. 1 and Fig. 1, where the cross section are assumed to be the RTA model, we numerically compare the stability for the split and the unsplit methods using the initial conditions as

$$r(x,\vec{v},0)=\left(1+\frac{e^{-v_1}+e^{v_1}}{2}\right)\mathscr{M}(\vec{v}),\quad j(x,\vec{v},0)=\frac{e^{-v_1}-e^{v_1}}{2\delta}\mathscr{M}(\vec{v}). \tag{4.3}$$

Table 1: Numerical stability condition for the split method in Example 1. Given the relation $\Delta t=c_{\delta,\Delta x}\Delta x^2$ with the unknown constant $c_{\delta,\Delta x}\in\mathbb{R}^+$, Table. 1 presents a group of $c_{\delta,\Delta x}$ for the split scheme.

$\Delta x=1/N$	25	50	100	200	400	800
$\epsilon=10^{-1}$	1/2	1	1	1	1	1
$\epsilon=10^{-2}$	1/4	1/4	1/3	1/2	1	1
$\epsilon=10^{-3}$	1	1	1	1/2	1/5	1/3
$\epsilon=10^{-4}$	2	2	2	2	2	2
$\epsilon=10^{-6}$	2	2	2	2	2	2

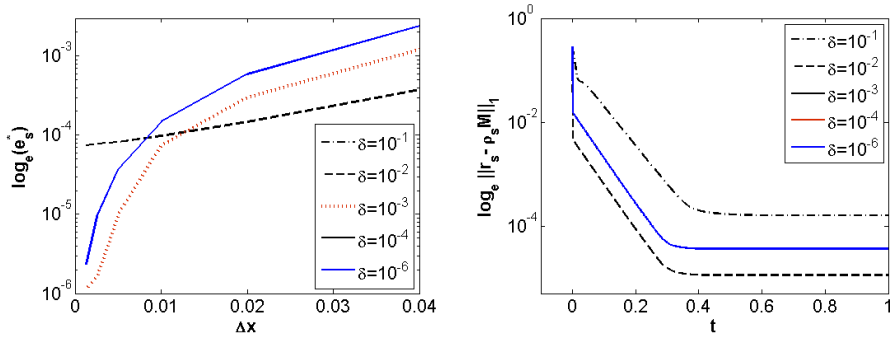

(a) Split Method

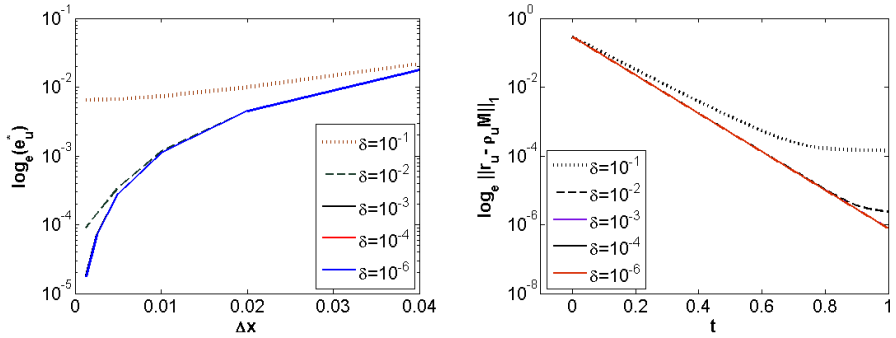

(b) Unsplit Method

Figure 1: Test of stability in Example 1. (a): left is the relation between Δt and Δx satisfies Table. 1. In the right one, the space step for $\|r_s - \rho_s \mathscr{M}\|_1$ is given as $\Delta x = 1/25$, and the time step satisfies Table. 1. (b): left is the relation between Δt and Δx satisfies $\Delta t = 2\Delta x^2$. In the right one, the space step for $\|r_u - \rho_u \mathscr{M}\|_1$ is given as $\Delta x = 1/25$ and the time step satisfies $\Delta t = 2\Delta x^2$.

There we assume $\delta \in \mathbb{R}_\delta = \{10^{-1}, 10^{-2}, 10^{-3}, 10^{-4}, 10^{-6}\}$, and set $\Delta x \in \mathbb{R}_{\Delta x} = \{1/25, 1/50, 1/100, 1/200, 1/400, 1/800\}$. We perform the comparison as follows. Given $\delta_0 \in \mathbb{R}_\delta$ and $\Delta x \in \mathbb{R}_{\Delta x}$, the constant $c_{\delta_0,\Delta x} \in \mathbb{R}^+$ in the relation $\Delta t = c_{\delta_0,\Delta x}\Delta x^2$ should be able to ensure the stability of the scheme when evolving the deviation $\|r_{s,u} - \rho_{s,u}\mathscr{M}\|_1$. Let c_{δ_0} be $c_{\delta_0} = \min_{\Delta x \in \mathbb{R}_{\Delta x}} c_{\delta_0,\Delta x}$. Then the scheme is uniform stable, w.r.t., Δx for δ_0 when $\Delta t = c_{\delta_0}\Delta x$. Similarly, let c be $c = \min_{\delta_0 \in \mathbb{R}_\delta} c_{\delta_0}$. The scheme is uniform stable, w.r.t., δ and Δx when $\Delta t = c\Delta x^2$.

In Table. 1, where the split method is applied, we present a group of the constant $c_{\delta_0,\Delta x}$. From the table, the split scheme is uniform stable, w.r.t., $\delta \in \mathbb{R}_\delta$ and $\Delta x \in \mathbb{R}_{\Delta x}$ when $\Delta t = \Delta x^2/5$. Additionally, the unsplit scheme is tested to be uniform stable, w.r.t., $\delta \in \mathbb{R}_\delta$ and $\Delta x \in \mathbb{R}_{\Delta x}$ when $\Delta t = 2\Delta x^2$. The numerical results are shown in Fig. 1, where we introduce $e^*_{\{s,u\}}$ for $\delta_0 \in \mathbb{R}_\delta$ and $\Delta x \in \mathbb{R}_{\Delta x}$ as

$$e^*_{\{s,u\}} = \sum_{k=1}^{K} \sum_{0 \le \mathbf{l} \le \mathbf{M}} |\varphi(x, \vec{v}^{\mathbf{l}}, t^k) - \rho_{s,u}(x, t^k))|\omega^{\mathbf{l}}\Delta t, \quad K = \left[\frac{T}{\Delta t}\right]. \tag{4.4}$$

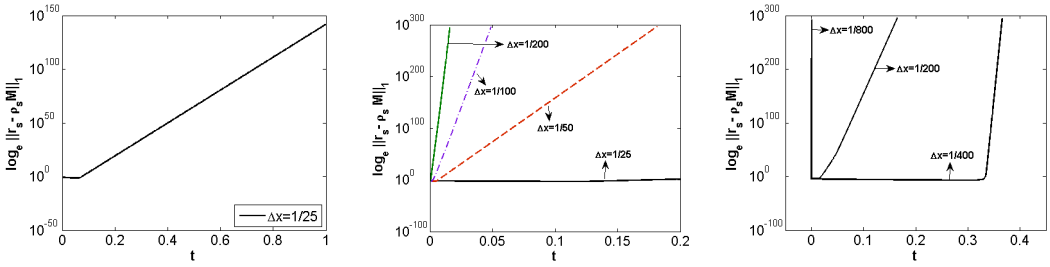

(a) $\epsilon = 10^{-1}$ (b) $\epsilon = 10^{-27}$ (c) $\epsilon = 10^{-3}$

Figure 2: Test of stability in Example 1. The evolution of $\|r_s - \rho_s \mathscr{M}\|_1$ in the three subfigures are solved with the split method. (a): with $\delta = 10^{-1}$ applied with $\Delta t = \Delta x^2$ for $\Delta x = 1/25$. (b): The evolution of $\|r_s - \rho_s \mathscr{M}\|_1$ with $\delta = 10^{-2}$ applied with $\Delta t = \Delta x^2/3$ for $\Delta x = 1/25$, $1/50$, $\Delta t = \Delta x^2/2$ for $\Delta x = 1/100$, and $\Delta t = \Delta x^2$ for $\Delta x = 1/200$. (c): with $\delta = 10^{-3}$ applied with $\Delta t = \Delta x^2$ for $\Delta x = 1/200$, $\Delta t = \Delta x^2/4$ for $\Delta x = 1/400$, and $\Delta t = \Delta x^2/2$ for $\Delta x = 1/800$.

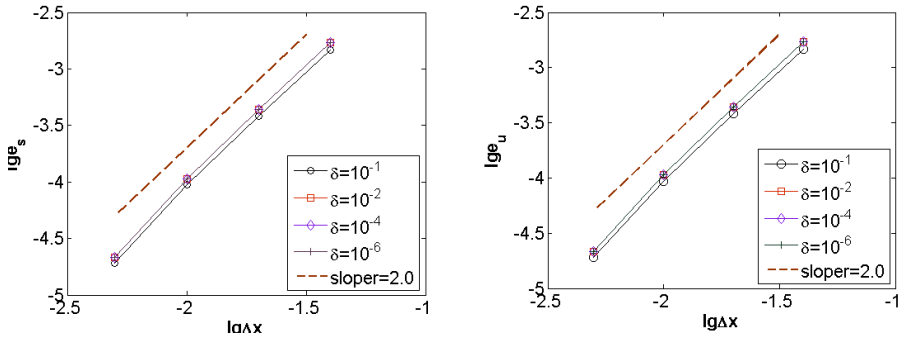

(a) Split Method (b) Unsplit Method

Figure 3: Test of convergence rate in Example 1. The relative error $e_{\{s,u\}}$ defined by (4.6) are solved with the split and unsplit methods, respectively.

Here the expansion form (3.4) of r is used. In Fig. 1(a), where the split method is applied, we solve e_s^* with $T = 1$ and present the numerical results in the left figure. There the mesh size is given by Table. 1. According to the numerical results, e_s^* decreases when Δx decreases. In other words, if the split scheme is stable with $\Delta x = 1/25$, then it is stable with any $\Delta x \in \mathbb{R}_{\Delta x}$. In the right figure in Fig. 1(a), we show the evolution of $\|r_s - \rho_s \mathscr{M}\|_1$ form $T = 0$ to $T = 1.0$ for $\delta_0 \in \mathbb{R}_\delta$ with $\Delta x = 1/25$. In Fig. 1(b), we repeat the computations in Fig. 1(a) using the unsplit method and the mesh size $\Delta x \in \mathbb{R}_{\Delta x}$, $\Delta t = 2\Delta x^2$. Furthermore, it can be seen in Fig. 2 that the split scheme is not uniform stable, w.r.t., $\Delta x \in \mathbb{R}_{\Delta x}$ and $\delta \in \mathbb{R}_\delta$ when $\Delta t = \Delta x^2/4$. There we recompute the deviation $\|r_s - \rho_s \mathscr{M}\|_1$ for $\delta = 10^{-1}$ using $\Delta x = 1/25$ with $c = 1$, for $\delta = 10^{-2}$ using $\Delta x = 1/25$, $1/50$ with $c = 1/3$, using $\Delta x = 1/100$ with $c = 1/2$, and using $\Delta x = 1/200$ with $c = 1$, for $\delta = 10^{-3}$ using $\Delta x = 1/200$ with $c = 1$, using $\Delta x = 1/400$ with $c = 1/4$, and using $\Delta x = 1/800$ with $c = 1/2$. As a conclusion, the unsplit method has a better numerical stability than the split method.

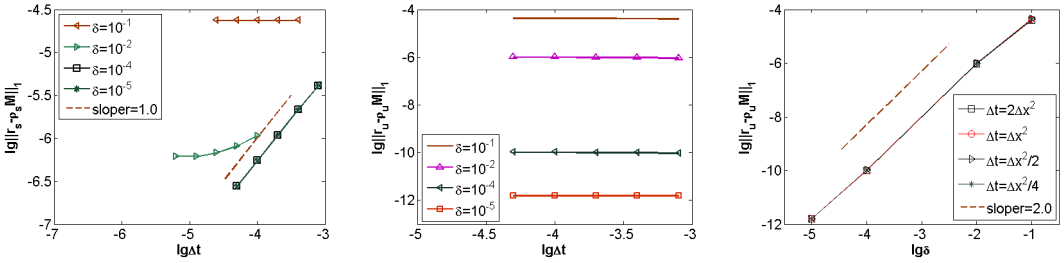

(a) Split Method (b) Unsplit Method

Figure 4: Test of feature (iii) in Example 1 with $T = 1$. The numerical results in (a) are solved with the split method and (b) are solved with the unsplit method.

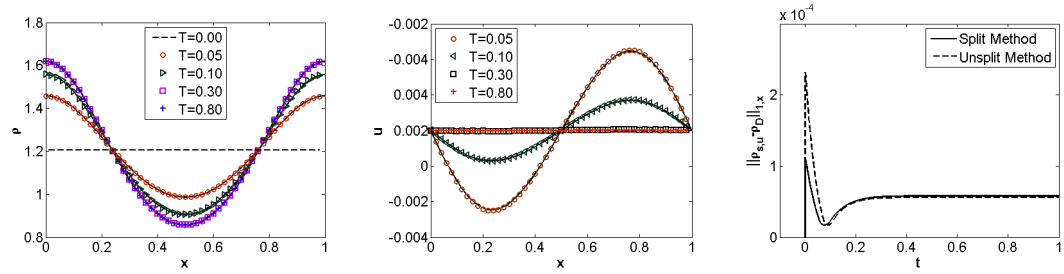

(a) Evolution of ρ and u (b) Evolution of $\|\rho_{s,u} - \rho_D\|_{1,x}$

Figure 5: Example 1. (a): the left describes the evolution of the mass density, with the dash line denoting the initial mass density. The right one gives the evolution of the bulk momentum, with the initial bulk velocity $u = 0$. (b): the evolution of $\|\rho_{s,u} - \rho_D\|_{1,x}$ from $T = 0$ to $T = 1.0$.

In the following computations, the cross section are all assumed to be as the mixture of RTA and EPI model, i.e., (4.1), and the initial conditions all have the forms of

$$r(x,\vec{v},0) = \left(0.5 + e^{-v_1^2}\right)\mathcal{M}(\vec{v}), \quad j(x,\vec{v},0) = 0\,. \tag{4.5}$$

In Fig. 3, where $\delta \in \mathbb{R}_{2,\delta} = \{10^{-1}, 10^{-2}, 10^{-4}, 10^{-6}\}$, we show the convergence rates of the two methods as follows. For a given $\delta \in \mathbb{R}_{2,\delta}$, we let the space step be $\Delta x \in \mathbb{R}_{2,\Delta x} = \{1/25, 1/50, 1/100, 1/200, 1/400\}$, and then chose the time step satisfying $\Delta t \sim O(\Delta x^2)$ in the condition of stability. In Fig. 3(a), where the split method is applied, we let $\Delta t = 1/400^2$ for $\delta = 10^{-1}, 10^{-2}$, and $\Delta t = 2/400^2$ for $\delta = 10^{-4}, 10^{-6}$. In Fig. 3(b), where the unsplit method is applied, we fix $\Delta t = 2/400^2$ for $\delta \in \mathbb{R}_{2,\delta}$ with $\Delta x \in \mathbb{R}_{2,\Delta x}$. Next, we solve $r_{s,u}$ at $T = 0.1$ and consider $\tilde{r}_{s,u}$ as the "reference" solution. Here $\tilde{r}_{s,u}$ is actually $r_{s,u}$ applied with $\Delta x = 1/400$. Finally, we solve the relative error $e_{\{s,u\}}$ through

$$e_{\{s,u\}} = \|r_{s,u} - \tilde{r}_{s,u}\|_1\,. \tag{4.6}$$

According to the numerical results, both of the split and the unsplit schemes are shown to be about second order, w.r.t., Δx, i.e., the feature (ii).

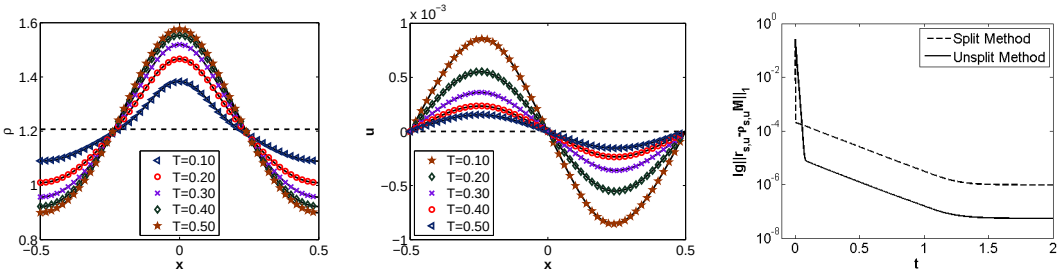

(a) Evolution of mass density. (b) Evolution of bulk momentum. (c) Evolution of $\|r_{s,u} - \rho_{s,u}\mathscr{M}\|_1$.

Figure 6: Numerical results for Example 2 with $\delta_0 = 10^{-3}$, and $\epsilon_0 = \frac{1}{250}$.

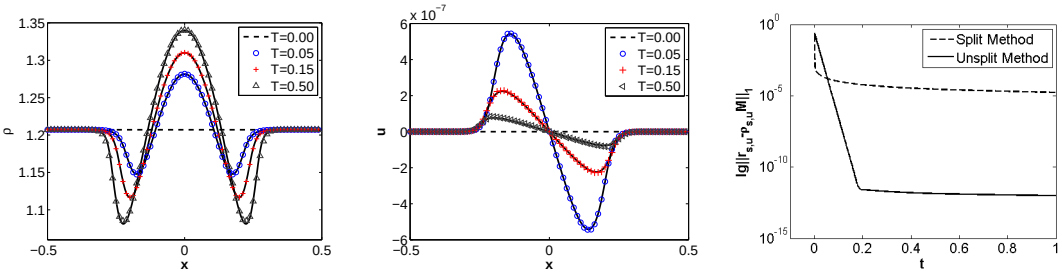

(a) Evolution of mass density (b) Evolution of bulk momentum (c) Evolution of $\lg\|r_{s,u} - \rho_{s,u}\mathscr{M}\|_1$

Figure 7: Numerical results for Example 2 with $\delta_0 = 0$, and $\epsilon_0 = 10^{-5}$.

In Fig. 4, where $\delta \in \{10^{-1}, 10^{-2}, 10^{-4}, 10^{-5}\}$, we solve the deviation $\|r_{s,u} - \rho_{s,u}\mathscr{M}\|_1$ at $T = 1.0$ with the fixed space step as $\Delta x = 1/50$. In the split method, we set $\Delta t = \Delta x^2/2^k$ with $k = 0, 1, 2, 3, 4$, for $\delta = 10^{-1}$, $k = 2, 3, 4, 5, 6$, for $\delta = 10^{-2}$, and $k = -1, 0, 1, 2, 3$, for $\delta = 10^{-4}, 10^{-5}$. In the unsplit method, we fix $\Delta t = 2\Delta x^2$ for all δ. In Fig. 4(a), where the split method is applied, the deviation $\|r_s - \rho_s\mathscr{M}\|_1$ is about first order, w.r.t., Δt when $\delta \ll 1$ and $\Delta t \gg \delta^2$. In Fig. 4(b), the left figure shows that $\|r_u - \rho_u\mathscr{M}\|_1$ is nearly independent of Δt, whereas, the right one suggests that $\|r_u - \rho_u\mathscr{M}\|_1$ is about second order, w.r.t., δ.

In Fig. 5, we assume $\delta = 0.005$. In Fig. 5(a), we present the evolutions of the mass density and the bulk momentum for the system. There the markers are solved by the unsplit method using the mesh size $\Delta x = 1/50$ and $\Delta t = 2\Delta x^2$. The solid lines denote the reference solutions. Since the split method applied with the same coarse grids coincides with the reference solutions well, thus we omit it here. In Fig. 5(b), we verify equation (2.9) and compare $\rho_{s,u}$ with ρ_D through the evolution of $\|\rho_{s,u} - \rho_D\|_{1,x}$ from $T = 0$ to $T = 1.0$. There, the space step is fixed as $\Delta x = 1/200$. The time steps for ρ_u and ρ_D satisfy $\Delta t = \Delta x^2$. The time step for ρ_s fulfils $\Delta t = \Delta x^2/4$. Moreover, the numerical tests show that the split scheme is unstable with $\Delta x = 1/200$ even when $\Delta t = \Delta x^2/2$.

Example 2. In this example, we consider a mixing regime, i.e.,

$$\epsilon(x) = \delta_0 + \epsilon_0 \exp(-100x^2).$$

in the computational domain $x \in [-0.5, 0.5]$. Here δ_0 and ϵ_0 are two constants. We still consider the mixture model (4.1). The electric field and the initial condition are as same as (4.2) and (4.5), respectively. According to the example, the two schemes are efficient for the mixing regime, too. The numerical results are shown in Fig. 6- 7.

In Fig. 6, we set $\delta_0 = 10^{-3}$ and $\epsilon_0 = 4 \times 10^{-3}$. There Fig. 6(a)-Fig. 6(b) describe the evolution of the mass density and the bulk momentum, respectively. The markers are solved with the unsplit method using $\Delta x = 1/50$ and $\Delta t = 2\Delta x^2$. The solid lines denote the reference solutions. In Fig. 6(c), we present the evolution of $\|r_{s,u} - \rho_{s,u}\mathscr{M}\|_1$ from $T = 0$ to $T = 2.0$. The solid line is solved with the unsplit method using $\Delta x = 1/50$ and $\Delta t = 2\Delta x^2$. The dash line is given with the split method using $\Delta x = 1/50$ and $\Delta t = \Delta x^2/2$. According to the numerical tests, the split scheme is unstable with $\Delta t = \Delta x^2$ when $\Delta x = 1/50$.

In Fig. 7, we set $\delta_0 = 0$ and $\epsilon_0 = 10^{-5}$. Similarly, we firstly present the evolutions of the mass density and the bulk momentum in Fig. 7(a) and Fig. 7(b), respectively. There the markers are solved with the unsplit method using $\Delta x = 1/80$ and $\Delta t = 2\Delta x^2$. The solid lines denote the reference solutions. In Fig. 7(c), we give the evolution of $\|r_{s,u} - \rho_{s,u}\mathscr{M}\|_1$ from $T = 0$ to $T = 1.0$. There both the solid line (which is solved with the unsplit method) and the dash line (which is solved with split method) are applied with the mesh size $\Delta x = 1/50$ and $\Delta t = 2\Delta x^2$. Differing from Fig. 6, the split scheme is stable in this situation even when $\Delta t = 2\Delta x^2$.

5. Conclusion

This paper derives the split and the unsplit schemes for the linear semiconductor Boltzmann equation with a diffusive scaling. The key point of the two schemes is rewriting the kinetic equation into the diffusive relaxation system, and applying the “BGK"-penalty method to the collision term. Through the numerical results, the two methods are shown to be asymptotic preserving. Furthermore, compared to the split method, the unsplit method has a better numerical stability than the split method.

Acknowledgments This research is supported by NSFC-10971115. I am grateful to S. Jin for helpful discussions and suggestions. I also thank the referee for his/her careful reading of the paper and constructive suggestions.

References

[1] N. B. Abdallah, P. Degond and S. Genieys, *An energy-transport model for semiconductors derived from the boltzmann equation*, J. Statist. Phys., vol. 84, no. 1-2 (1996), pp. 205–231.

[2] N. B. Abdallah, and P. Degond, *On a hierarchy of macroscopic models for semiconductors*, J. Math. Phys., vol. 37, no. 7 (1996), pp. 3306–3333.

[3] G. Bal and Y. Maday, *Coupling of transport and diffusion models in linear transport theory*, Math. Model. Numer. Anal., vol. 36, no. 1(2002), pp. 69–86.

[4] C. Cercignani, *The Boltzmann Equation and Its Appliccations*, Springer, Berlin, Wien, 1998.

[5] P. DEGOND AND S. JIN, *A smooth transition model between kinetic and diffusion equations*, SIAM. J. Numer. Anal., vol. 42, no. 6 (2005), pp. 2671–2687(electronic).
[6] F. FILBET AND S. JIN, *A class of asymptotic preserving schemes for kinetic equations and related problems with stiff sources*, J. Comput. Phys.,vol. 229, no. 20 (2010), pp. 7625–7648.
[7] F. GOLSE, S. JIN AND C. D. LEVERMORE, *A Domain Decomposition Analysis for a Two-Scale Linear Transport Problem*, Math. Model. Numer. Anal., vol. 37, no. 6 (2003), pp. 869–892.
[8] J. HU AND S. JIN, *On kinetic flux vector splitting schemes for quantum euler equations, kinetic and related models*, Kinetic and Related Models., vol. 4, no. 2 (2011), pp. 517–530.
[9] S. JIN, *Efficient asymptotic-preserving (AP) schemes for some multiscale kinetic equations*, SIAM J. Sci. Comput., vol. 21, no. 2 (1999), pp. 441–454.
[10] S. JIN AND L. PARESCHI, *Discretization of the multiscale semiconductor boltzmann equation by diffusive relaxation schemes*, J. Comput. Phys., vol. 161, no. 1 (2000), pp. 312–330.
[11] S. JIN, L. PARESCHI AND G. TOSCANI, *Diffusive relaxation schemes for multiscale discrete velocity kinetic equations*, SIAM J. Numer. Anal., vol. 35, no. 6 (1998), pp. 2405–2439 (electronic).
[12] S. JIN, L. PARESCHI AND G. TOSCANI, *Asymptotic-preserving (AP) schemes for multiscale kinetic equations: a unified approach*, Hyperbolic problems: theory, numerics, applications, Vol. I, II (Magdeburg, 2000), 573ÍC582, Internat. Ser. Numer. Math., 140, 141, Birkhäuser, Basel, 2001.
[13] S. JIN AND B. YAN, *A class of asymptotic-preserving schemes for the fokker-planck-landau equation*, J. Comput. Phys., vol. 230, no. 17 (2011), pp. 6420–6437.
[14] A. KLAR, *Asymptotic-induced domain decomposition methods for kinetic and drift diffusion semiconductor equations*, SIAM J. Sci. Comput., vol. 19, no. 6 (1998), pp. 2032–2050 (electronic).
[15] C. D. LEVERMORE, *Moment closure hierarchies for kinetic theories*, J. Statist. Phys., vol. 83, no. 5-6 (1996), pp. 1021–1065.
[16] R. LEVEQUE, *Numerical Methods for Conservation Laws*, Birkhäuser Verlag, Basel, 1992.
[17] P. A. MARKOWICH, C. A. RINGHOFER AND C. SCHMEISER, *Semiconductor Equations*, Springer-Verlag Wien, New York, 1990.
[18] C. SCHMEISER AND A. ZWRICHMAYR, *Convergence of moment methods for linear kinetic equations*, SIAM J. Numer. Anal., vol. 36, no. 1 (1999), pp. 74–88.
[19] C. RINGHOFER, C. SCHMEISER AND A. ZWRICHMAYR, *Moment methods for the semiconductor Boltzmann equation on bounded position domains*, SIAM J. Numer. Anal., vol. 39, no. 3 (2002), pp. 1078–1095.
[20] M. TIDRIRI, *New models for the solution of intermediate regimes in transport theory and radiative transfer: Existence theory, positivity, asymptotic analysis and approximations*, J. Statist. Phys., vol. 104, no. 1-2 (2001), pp. 291–325.